Wood Physics/Mechanical Properties

Mojgan Vaziri*, Christopher Dreimol, Lars Abrahamsson, Peter Niemz and Dick Sandberg

Parameter estimation and model selection for water vapour sorption of welded bond-line of European beech and Scots pine

https://doi.org/10.1515/hf-2022-0013
Received January 21, 2022; accepted April 11, 2023;
published online June 9, 2023

Abstract: The single exponential kinetics (SEK) and parallel exponential kinetics (PEK) models were fitted to kinetic sorption data of welded and unwelded Scots pine (*Pinus sylvestris* L.) and European beech (*Fagus sylvatica* L.). Furthermore, diffusion coefficients of water vapour in wood were determined using two different Fickian diffusion solutions. The objective was to identify how well these models could represent the moisture contents of the specimens and to characterize differences between the sorption behaviour of welded and unwelded wood. This knowledge can be used to enhance the moisture resistance of welded wood, develop drying schedules, and improve the quality of timbers. The PEK and SEK models provided the most precise and the second most precise fits to the sorption kinetic data, respectively. The two Fickian models are equivalent when both the infinite series are truncated at $n = 10$. The Fickian models also exhibited the highest discrepancy with the experimental data. Nevertheless, the Fickian models fit relatively better to the sorption data of the welded wood than to that of the unwelded wood. This behaviour may be due to the rigid and less-swelling structure of the welded bond line.

Keywords: DVS; Fick; PEK; SEK; sorption kinetics.

***Corresponding author: Mojgan Vaziri**, Wood Science and Engineering, Luleå University of Technology, Forskargatan 1, 931 87 Skellefteå, Sweden, E-mail: mojgan.vaziri@ltu.se
Christopher Dreimol, Wood Materials Science, Institute for Building Materials, ETH Zürich, 8093 Zürich, Switzerland; and Cellulose & Wood Materials Laboratory, Empa, 8600 Dübendorf, Switzerland
Lars Abrahamsson, Vattenfall AB, BU Fuel, Engineering & Projects, Evenemangsgatan 13, 169 79 Solna, Sweden
Peter Niemz, Wood Materials Science, Institute for Building Materials, ETH Zürich, 8093 Zürich, Switzerland
Dick Sandberg, Wood Science and Engineering, Luleå University of Technology, Forskargatan 1, 931 87 Skellefteå, Sweden

1 Introduction

1.1 Wood welding and water sorption

The studies related to structural applications of welded wood are few in part due to the vulnerability of the welded joint to damage from moisture (Vaziri 2011). Enhancing the water resistance of the welded joint requires a full understanding of the water sorption mechanism, and the present study contributes to increasing this knowledge.

Since the 1980s, the dynamic vapour sorption (DVS) technique has been used to characterize the sorption isotherms where the time-dependent changes in the mass for different steps of relative humidity (RH) are recorded. The sorption data are usually used for fitting against advanced computer-based kinetic models. Recently, considerable progress has been made regarding the understanding and modelling of moisture transport processes in wood (Glass et al. 2018; Thybring et al. 2019a; Zelinka et al. 2018). These models are based on analytical expressions and a few parameters that need to be estimated by inverse analysis.

The sorption kinetics data of wood are often interpreted by a Fickian diffusion law (Jalaludin et al. 2010; Papadopoulos and Hill 2003; Pfriem et al. 2010; Salin 2010). Fick (1855) was the first who made this kind of modelling possible by placing diffusion on a quantitative basis (Avramidis 2007). Thybring et al. (2019b) reviewed a handful of popular and recent theoretical models.

The parallel exponential kinetic (PEK) model has been comparatively recently introduced to the wood science literature. The PEK model, first proposed for cellulosic materials by Kohler et al. (2003, 2006), is an extension of a single kinetic exponential model (SEK) (Glass et al. 2017). It has been found that the PEK model provides precise fits to the sorption kinetic data of natural fibres (Belbekhouche et al. 2011; Hill et al. 2010a; Kohler et al. 2003; Xie et al. 2011), regenerated cellulose (Okubayashi et al. 2004; 2005a, b), and wood (Hill et al. 2010b, 2010c; Jalaludin et al. 2010; Popescu and Hill 2013; Popescu et al. 2014; Sharratt et al. 2010).

Abundant speculations have been derived from PEK model parameters that mainly are based upon the assumption

that the model consists of two processes: (1) a fast process associated with the monolayer formation of strongly bound water to the polar groups within the cell wall, and (2) a slow process associated with the water sorption to the multilayer of weakly bound water in the larger water clusters (Kohler et al. 2003, 2006). However, none of the claims is experimentally proven, and it is not yet clear what these two processes represent (Hill et al. 2010d; Xie et al. 2011).

Thybring et al. (2019a) showed by multi-exponential decay analysis (MEDEA) that the sorption kinetic data to equilibrium frequently contains more than two characteristic exponential components. Glass and co-workers (Glass et al. 2017, 2018; Thybring et al. 2019a) claimed that fitting PEK to the sorption kinetic data severely mischaracterizes both the equilibrium moisture content (EMC) and the full kinetic behaviour. Therefore, the PEK model cannot be used to derive physically meaningful properties from water vapour sorption measurements.

On the other hand, the degree of accuracy that Glass and co-workers expect from DVS experiments seems idealistic, especially for a complex hygroscopic polymer such as wood. Furthermore, considering the above-mentioned material properties making such a conclusion must be supported by a much larger data set than only one sample.

To the best of our knowledge, this is the first study in which the time-dependent transition of MC after a stepwise change in RH from one level to another (i.e., sorption kinetics) of welded wood has been studied. The purpose of this study was to compare the sorption behaviours of welded and unwelded wood at the same experimental conditions rather than to characterize moisture content (MC) accurately.

2 Materials and methods

2.1 The experiment

In this work, the welded and unwelded Scots pine (*Pinus sylvestris* L.) and European beech (*Fagus sylvatica* L.) were studied, and the experimental procedure is described in detail in Vaziri et al. (2023).

Considering Glass and co-workers' recommendation (Glass et al. 2017), the stop criterion (dm/dt) used in this study was more straightened than the usual standard (60 min hold time or change in moisture content <0.002 % min^{-1} over a 10 min period) and identical to the stop criterion used by Grönquist et al. (2019). Equilibrium in each step was defined to be attained at a mass change per time (dm/dt) of less than 0.0005 % min^{-1} over a 10 min window or a maximum time of 1000 min per step. The latter criterion never needed to be triggered. The maximal sorption time was 775.67 min for one welded beech specimen in an adsorption step from 85 % to 95 % RH.

The specimens were cut with identical dimensions, but due to the rigidity of the welded wood, some specimens got irregular edges, which could be one of the error sources in the DVS experiment.

It should be considered that errors in EMC measurement with DVS are associated with error sources such as stop criterion, weighing of samples, dimensional measurement of samples, temperature, RH control, etc. Some of these uncertainties in EMC measurements are discussed by Berger et al. (2020), Glass et al. (2018), Willems (2022), and Zelinka et al. (2018).

2.2 Diffusion problems – or Fick's law

The theoretical background to Fickian diffusion of this paper is mainly relying on Crank (1975). Many recent publications inaccurately cite the works of Crank. Therefore, going back to the original source is preferable.

2.2.1 Some theoretical background: Diffusion of water in wood refers to the molecular movement of bound water through the gross wood system by transferring through the cell-wall substance and lumen void volume from a higher water concentration area to a lower one (Avramidis 2007).

The diffusion coefficient can be either constant or dependent upon the concentration, pressure, temperature, and composition of the medium (Crank 1975). In general, the diffusion coefficients of wood are a function of the above-mentioned factors and the method of their determination (Keey et al. 1999; Stamm 1964).

If no dimensional changes occur in wood, the diffusion coefficient D ($m^2\,s^{-1}$) is constant. Making further simplifications (Section 4.3.2 in Crank 1975), two different solutions can be derived for an infinitely wide plane sheet. The exact details of solving these problems can be found in Section 4.3 in Crank (1975) and the references mentioned in that section. The general theory about diffusion-equation solving can be found in e.g., Sparr and Sparr (2000).

The diffusion problem is defined as

$$\frac{\partial C}{\partial t} = D\frac{\partial^2 C}{\partial x^2} \tag{1}$$

where, C denotes the concentration of water in the specimen, t time, and x the thickness direction of the sheet. Given that C_1 is the concentration of water at the surfaces as well as of the entire specimen in steady-state, and C_0 denotes the initial concentration of water in the entire specimen before the stepwise RH change, the relative change of water concentration can be expressed as $\frac{C(t,x)-C_0}{C_1-C_0}$.

Concentration is hard to measure, but the mass of the specimen can be measured in the DVS. The relative mass change of the diffusing water and the relative concentration change of it is however equivalent. Integrating the space-dependent

$$\frac{M(t,x)-M_0}{M_1-M_0} = \frac{C(t,x)-C_0}{C_1-C_0} \tag{2}$$

over specimen thickness $x \in \{-L, L\}$ reveals

$$E(t) = \frac{M(t)-M_0}{M(\infty)-M_0} \tag{3}$$

where E denotes the fractional change in moisture content of the wood, M_0 (mg) is the mass of the specimen before the RH step change, $M(\infty)$ (mg) is the mass at equilibrium.

2.2.2 The two Fickian-based models of fractional change in moisture content, E(t): In Crank (1975) two alternative solution forms of Equation (3) are presented. Both solutions to the partial differential equation

are in the forms of infinite series. One solution is more accurate for short times, whereas the other one is more accurate for long times for finite numbers of series components. For $n \to \infty$ one would expect the solutions to be equal even if it is not explicitly stated in Crank (1975), and one of them is based upon a space-time independency assumption. This paper wanted to show that the solutions are similar already when cutting the series after $n = 10$.

The first of the two solutions which is determined by the method of separation of variables (space and time) yields

$$E(t) = \frac{M(t) - M_0}{M(\infty) - M_0} = 1 - \sum_{n=0}^{\infty} \frac{8}{(2n+1)^2\pi^2} \mathrm{e}^{\left(\frac{-(2n+1)^2\pi^2}{4L^2} Dt\right)} \quad (4)$$

where, L is half of the thickness of the specimen (Equation 4.18, Crank 1975). The solution of Equation (4) is more accurate for long times, i.e., times close to when steady state has been reached and when the diffusion process starts to decay.

The second solution which can be achieved using the Laplace transform yields

$$E(t) = \frac{M(t) - M_0}{M(\infty) - M_0} = 2\sqrt{\frac{Dt}{L^2}}\left(\frac{1}{\sqrt{\pi}} + 2\sum_{n=1}^{\infty} (-1)^n \mathrm{ierfc}\left(\frac{nL}{\sqrt{Dt}}\right)\right) \quad (5)$$

is more accurate for short times (Equation 4.18, Crank 1975), i.e., right after the diffusion process has started from a steady-state condition after a stepwise change in RH.

It is not precisely stated in Crank (1975) for which time intervals the two different solutions are valid for a given n where the series are cut off. In this paper it is shown that for a low n-number both solutions are replaceable.

2.2.3 The simplified versions of MC(t) used for plotting and root-mean-square error (RMSE) estimations: For expressing $\mathrm{MC}(t)$ using the time series of $E(t)$

$$MC(t) = \frac{M(t) - M_0}{M_0} = E(t)\frac{(M(\infty) - M_0)}{M_0} \quad (6)$$

can be used.

For full accuracy, the entire series of Equations (4) and (5) should be used. It is common in the literature to cut the series already at $n = 1$, but in this paper for more accuracy the infinite series were truncated at $n = 10$ for both the short-time and long-time Fickian-based approaches.

2.2.4 Determination of the diffusion coefficients: In this paper, the diffusion coefficients were assumed to be constant for each RH step and therefore were determined for each of the RH steps.

For the short times model – the initial rates of sorption and desorption (ISORAD) method determining D is described in Vaziri et al. (2023). The numerical values regardless of the method are similar as seen in Equations (8)–(10). This is according to the theory on p. 245, Crank (1975).

The method for determining D in this paper (using the long-times model) is very simplistic and it takes

$$E(t) \approx 1 - \frac{8}{\pi^2}\mathrm{e}^{\frac{-\pi^2 tD}{4L}}, \quad (7)$$

which is Equation (4) truncated at $n = 0$, and solves it for

$$D = \frac{4L^2}{\pi^2 t_{\frac{1}{2}}}\ln\left(\frac{16}{\pi^2}\right) \approx \frac{0.1958L^2}{t_{\frac{1}{2}}}, \quad (8)$$

knowing $t_{\frac{1}{2}}$ from the measurement data, where $t_{\frac{1}{2}}$ is defined by $E\left(t_{\frac{1}{2}}\right) = \frac{1}{2}$.

For numerical comparison, the ISORAD method results in

$$D = \frac{\pi}{16\left(\frac{t_{\frac{1}{2}}}{L^2}\right)} \approx \frac{0.1963L^2}{t_{\frac{1}{2}}}, \quad (9)$$

and the sorption method which was proposed in Section 10.6.5, Equation (10.158), Crank (1975) results in

$$D = -\frac{4L^2}{\pi^2 t_{\frac{1}{2}}}\ln\left(\frac{\pi^2}{16} - \frac{1}{9}\left(\frac{\pi^2}{16}\right)^9\right) \approx \frac{0.1967L^2}{t_{\frac{1}{2}}}. \quad (10)$$

2.3 The exponential models

2.3.1 The parallel exponential kinetics (PEK) model: The PEK model is expressed as

$$\mathrm{MC}(t) = \mathrm{MC}_0 + \mathrm{MC}_1\left(1 - \mathrm{e}^{-\frac{t}{t_1}}\right) + \mathrm{MC}_2\left(1 - \mathrm{e}^{-\frac{t}{t_2}}\right) \quad (11)$$

where $\mathrm{MC}(t)$ denotes the moisture content of the sample at time t, and MC_0 is ideally the MC of the sample at time zero. The two exponential terms, $\left(\mathrm{MC}_1\left(1 - \mathrm{e}^{-\frac{t}{t_1}}\right)\right)$ and $\left(\mathrm{MC}_2\left(1 - \mathrm{e}^{-\frac{t}{t_2}}\right)\right)$ represent the fast and slow processes, respectively. The two processes are taking place simultaneously.

Equilibrium moisture content (EMC) is theoretically defined as

$$\mathrm{MC}(\infty) = \mathrm{MC}_0 + \mathrm{MC}_1 + \mathrm{MC}_2, \quad (12)$$

but the exact values of MC_1 and MC_2 must be determined through several measurements of $\mathrm{MC}(t)$. Moreover, t never reaches ∞ in real life.

2.3.2 The single exponential kinetics (SEK) model: SEK is a simplified version of the PEK model with only one exponential term:

$$\mathrm{MC}(t) = \mathrm{MC}_A + \mathrm{MC}_B\left(1 - \mathrm{e}^{-\frac{t}{\tau}}\right) \quad (13)$$

where MC_A is the MC of the sample at time 0. Analogously with the PEK case, $\mathrm{MC}_A + \mathrm{MC}_B$ represents the EMC, and τ denotes the characteristic time constant.

The idea of testing this model was to see if there is an artificial compromise exponential process that can mimic the two physical exponential processes behind PEK in a "good-enough" manner.

2.4 The fitting procedure

Curve fitting was performed in MATLAB® R2020a (Mathworks, Natick, Massachusetts, USA) using the in-built fit function for non-weighted and non-linear least-squares fitting.

The input data for fitting the PEK and SEK models consisted of experimental data of time t (min), MC (%), and a binary parameter determining whether the fit was about adsorption or desorption. The "Non-linear Least-Squares" method and the "Trust-Region" algorithm were used for both models. The maximal number of function evaluations and iterations was set to 5000 in both cases.

Due to the limitations of the curve-fitting function in Matlab, one cannot easily create a model that automatically makes sure that:

$$t_1 \leq t_2 \tag{14}$$

and, in turn, automatically determines a breaking point between the two parameters. This had to be implemented manually by introducing the variable limits

$$0 \leq t_1 \leq 16 \tag{15}$$
$$16 \leq t_2 \leq 260 \tag{16}$$

to the algorithm. The numbers 16 and 260 were empirically chosen by experimenting combined with some engineering knowledge of the processes behind the equation. In alignment with Equations (15) and (16), the boundary condition

$$0 \leq \tau \leq 260 \tag{17}$$

was produced for the SEK fitting model.

For increasing RH values (adsorption), the exponential coefficients MC_1, MC_2, and MC_B of the PEK and SEK models are positive, whereas they are negative for decreasing RH values (desorption). The constant parts of both models (MC_0 and MC_A) were positively unbounded.

Figure 1 shows the data from the first 3.0 min of the experiment for 10 % RH. Due to the curvature of the fitting curves at the first minutes of the sorption, some approaches have removed these data points and shifted the time axis for better curve fitting (Glass et al. 2018; Hill et al. 2010c). The approach used here left these data and the time axis unaltered. Unlike Thybring et al. (2019b), the fitting in this study was done for all parameters to minimize the total residual of the curve against measurement data. In Thybring et al. (2019b, p. 727), on the other hand, MC_0 is manually set equal to the first value of the measured time series. That gives a zero residual at $t = 0$, but generally worse performance. In Figure 1, one can see that MC_0 is set by optimization and not manually since the fitted curve differs from the measurements in the initial time steps.

The starting point of the fitting algorithm was set to 1 for the PEK and SEK time constants τ, t_1, and t_2. The initial values of MC_0 and the PEK fitting coefficients, i.e., MC_1 and MC_2 were set to 0, regardless of whether the case fitted for is adsorbing or desorbing. For the SEK fitting, on the other hand, the iteration is initiated with 1 for the coefficient MC_B when adsorbing, whereas it is set to –1 when desorbing. Similarly, as for the PEK case, the starting point of the initial value MC_A is set to 0.

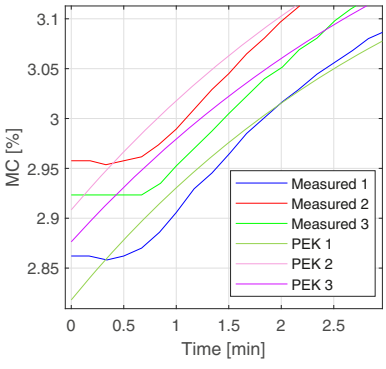

Figure 1: Fitting the PEK model to kinetic sorption data of three replicates of beech in adsorption at 10 % RH. The bends at the beginning of the curves are visible from 0 to 0.75 min.

The optional parameter "`DiffMinChange`" was set to 10^{-14} in the PEK fitting, whereas the default value was good enough for the SEK fitting. All these values were chosen by a combination of modelling knowledge and empiricism.

3 Results and discussion

In all results, the behaviours of the short-time and long-time Fickian models are almost identical all the time and for all specimens. The two Fickian models are equivalent when both the infinite series are truncated at $n = 10$. Some interesting examples are shown here for different RH steps, adsorbing and desorbing, comparing unwelded and welded wood. The examples are to some extent taken arbitrarily, since an all-embracing bouquet of representative figures would be unrealistic to produce for the paper.

The differences between pine and beech were so small that it could not be motivated showing similar examples for pine and welded pine as are already shown in Figures 2–5 for beech and welded beech.

3.1 Adsorption

3.1.1 RH 0 %–5 %

Figure 2 presents a typical example of the model fits to the kinetic sorption data in adsorption in an RH step of 0 %–5 % comparing beech and welded beech. In Figures 2A and B, the MC of beech and welded beech for RH 0 %–5 % are compared. The MC change is higher for beech than welded beech. The deviation in MC between the replicates is higher for welded beech than for beech. Such spread between the replicates can be seen also for welded pine but the spread is much smaller than for welded beech. It is not clear whether it is due to degradation of wood by welding or just that the variation in specimen's geometry is higher for welded wood.

Figures 2C and D show the prediction errors (residuals) for the first 50 min of the sorption process. The residuals are lower in absolute value for welded beech. Their characteristics also vary somewhat between welded beech and beech. From all these figures (especially Figure 2C and D) it can be seen that the SEK and PEK models provide better and different fits to the sorption data than the two Fickian models. For the unwelded wood case, SEK and PEK are identical, which also is verified by Appendix Figure A1.

Figures 3A and B focus on the later parts of the above given sorption process. For beech, the Fickian models fit better than the SEK and PEK to the sorption data at the end of this sorption step. For welded beech, PEK and the Fickian

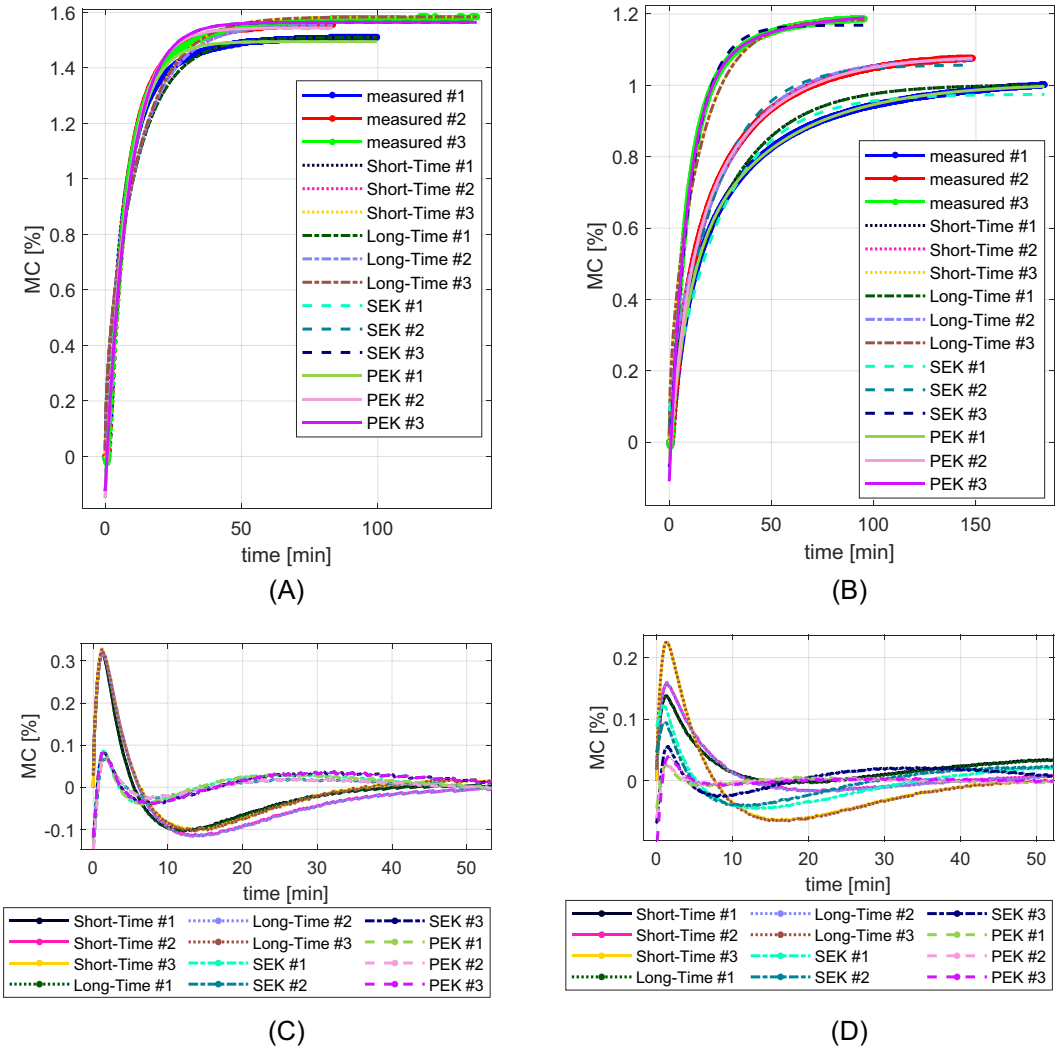

Figure 2: Moisture content of three replicates of beech and welded beech in adsorption from 0 %–5 % RH as a function of time with all model fits. (A) The whole sorption process at 0%–5% RH and the model fits for beech. (B) The whole sorption process at 0%–5% RH and the model fits for welded beech. (C) Residuals of the model fits at the first 50 min of the sorption process for beech. (D) Residuals of the model fits at the first 50 min of the sorption process for welded beech.

models equally fit better than SEK to the sorption data in the later parts of the sorption step.

Figures 3C and D illustrate the first 25 min of the sorption process. The SEK and PEK fit better than the Fickian models to the sorption data for both welded and unwelded beech.

3.1.2 RH 90 %–95 %

In Figure 2, all replicates start with the same MC level but later at 90 %–95 % RH in Figure 4, the spread between the replicates has increased throughout the experiment. For each stepwise change in RH, the deviation between the initial MC values of the three replicates increase further.

The MC is generally lower, and the MC increase is also smaller for welded beech in Figures 4A and B. The residuals of the model fits in Figures 4C and D are also lower for welded beech. Moreover, the residuals have completely different characteristics for welded wood, implying that other phenomena might lie behind the dynamic vapour sorption process of the welded joints than of untreated wood.

3.2 Desorption – RH 80 %–75 %

Figures 5A and B show desorption curves of welded and unwelded beech replicates for 80%–75 % RH. The Fickian

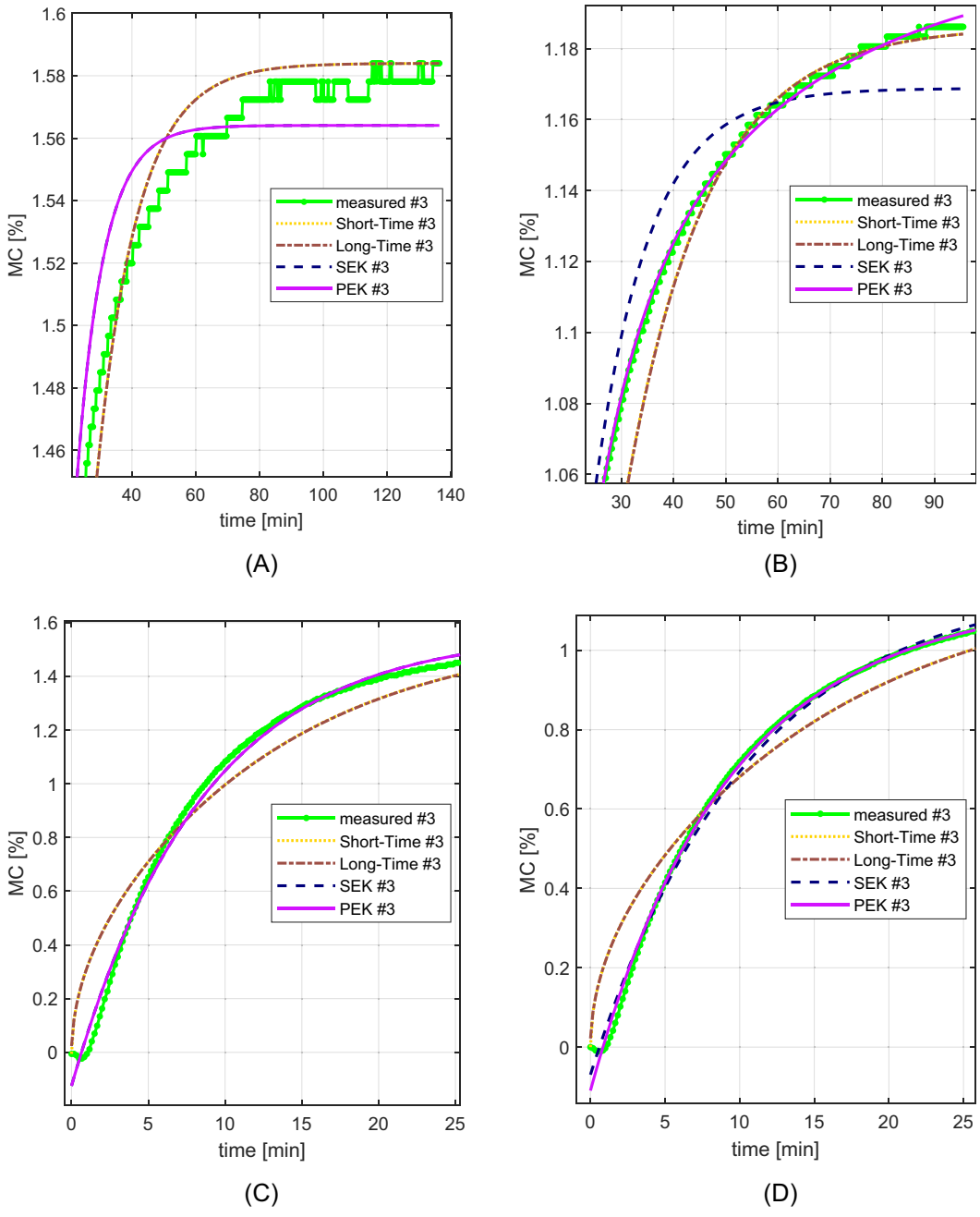

Figure 3: Moisture content as a function of time in adsorption at 0 %–5 % RH and their model fits for one replicate of welded and unwelded beech with focus on the beginning and end of the process. (A) Focus on one replicate at the end of the sorption process at 0%–5% RH for beech. Long-time and short-time Fickian curves overlap. SEK and PEK overlap. (B) Focus on one replicate at the end of the sorption process at 0%–5% RH for welded beech. Long-time and short-time Fickian curves overlap. (C) Model fits to the sorption data, truncated at first 25 min of sorption process for one replicate of beech. (D) Model fits to the sorption data, truncated at first 25 min of sorption process for one replicate of welded beech.

models overlap each other and deviate considerably from SEK and PEK which much better resemble the behaviour of the MC curves. SEK has however large residuals in the beginning. The Fickian and SEK challenges are common for desorption.

Figures 5C and D show the residuals of the first few minutes of the desorption process. The Fickian and PEK models reveal similar fits, but the SEK model does not fit precisely to the sorption curves, which is comparable to the Fickian long-term model truncated too early

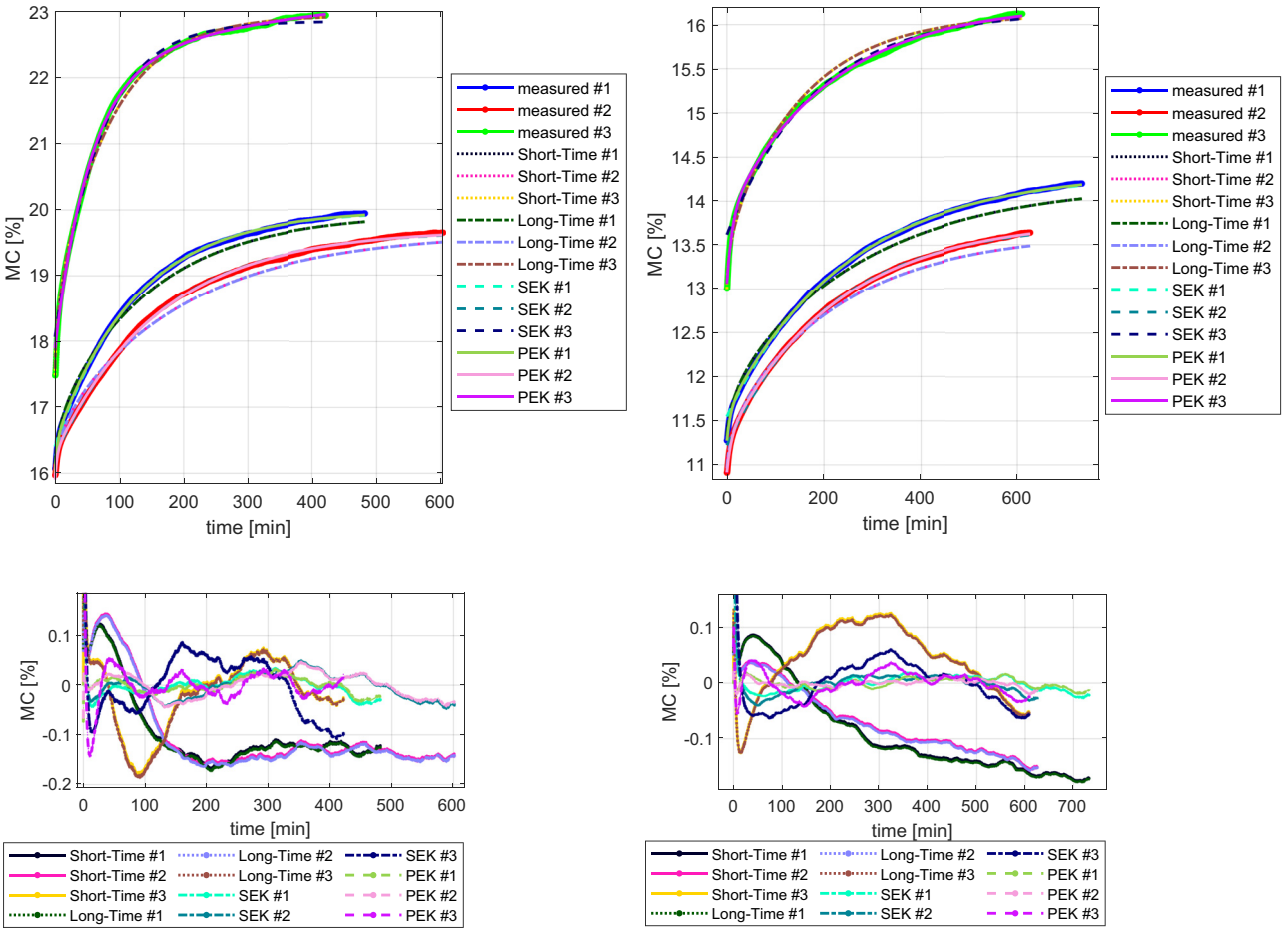

Figure 4: Moisture content of three replicates of beech and welded beech in adsorption from 90 %–95 % RH as a function of time with all model fits. (A) The whole sorption process at 90 %–95 % RH and the model fits for beech. (B) The whole sorption process at 90 %–95 % RH and the model fits for welded beech. (C) Residuals of the model fits for beech. (D) Residuals of the model fits for welded beech.

($n = 0$). As usual, the welded case has slightly smaller residuals.

Figures 5E and F show the residuals of the model fits for the entire desorption process. Focus is on the non-Fickian curves, disregarding the early large residuals of SEK. The residuals are similar for welded and unwelded beech at the beginning and end of the fits but differ in the middle in pattern. The SEK (ignoring the early stage) and PEK models provide precise fits to the welded and unwelded sorption kinetic data. The residuals of PEK do not exceed ±0.10 percentage points of MC (in the beginning, c.f. Figures 5E and F) and most of the time not more than 0.02 % percentage points. The Fickian models generally had a better fit to the sorption data in adsorption than desorption (Figures 2, 4, and 5 – and a summary in Figure 7).

3.3 Aggregating the results

Appendix Figure A1 shows that the SEK and PEK outperform the Fickian models. For most of the cases, the two Fickian models perform equivalently, whereas it is only in the 0 %–5 % RH step that SEK and PEK perform equivalently. PEK with more fitting parameters should in the general case provide a better fit than SEK.

All models have more challenges in higher RH and desorption, and combining high RH and desorption makes that even harder. This can be seen in Appendix Figures A1–A4 for the four different wood types, and in Figure 7 where an average is taken over the wood types.

Moreover, in Figure 6, one can see that the RMSEs of welded wood are in general smaller than those of unwelded wood. In addition to that, the RMSEs of pine and welded

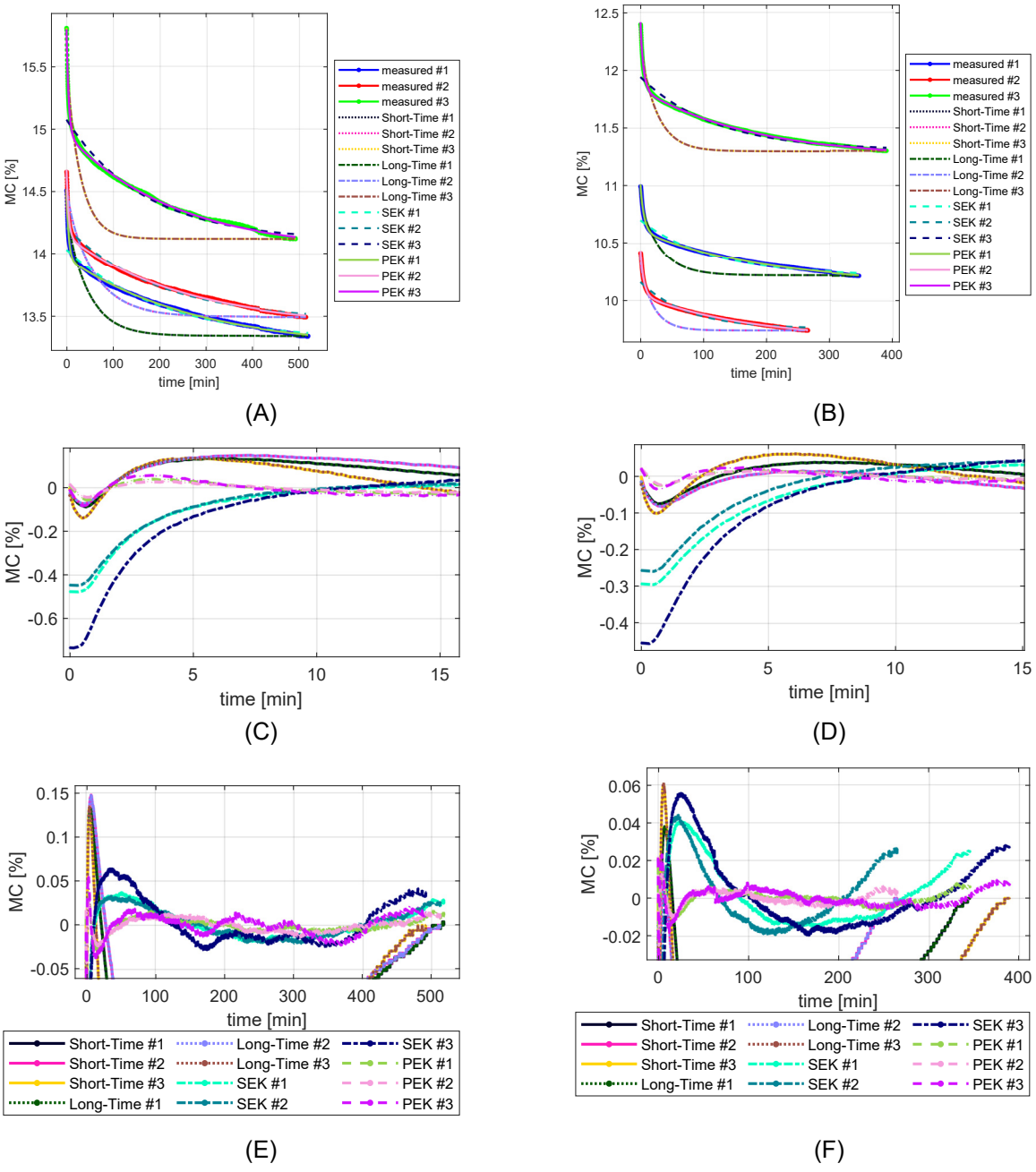

Figure 5: Moisture content of three replicates of beech and welded beech in desorption from 80 %-75 % RH as a function of time with all model fits. (A) The desorption process at 80 %-75 % RH and the model fits for beech. (B) The desorption process at 80 %-75 % RH and the model fits for welded beech. (C) Residuals of the first 15 min of the desorption process for beech with focus on SEK. (D) Residuals of the first 15 min of the desorption process for welded beech with focus on SEK. (E) Residuals through the desorption process for beech, ignoring the outliers. (F) Residuals through the desorption process for welded beech, ignoring the outliers.

pine are slightly higher than those of beech and welded beech. Welded wood seems to be more Fickian in its properties. One possible explanation is that the rigid structure of the welded bond line restricts its swelling. The diffusion behaviour of many swelling polymers such as wood cannot be explained by Fick's law with constant boundary conditions (Section 11.1, Crank 1975; Van der Wel and Adan 1999).

In Figure 7 the average RMSEs of all specimen types are shown for different stages of RH-targets. In that figure (and in Figure 6), the vertical axis is linear and not logarithmic as in Appendix Figures A1–A4. Having linear vertical axes for

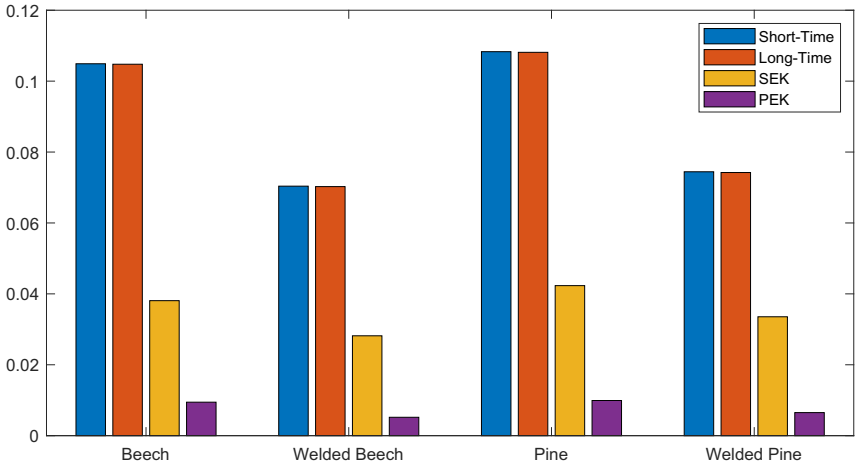

Figure 6: The average RMSEs values, over the three replicates and all RH targets, for each specimen type and the four different model fits. Welded wood is easier to represent by the models used. Pine is slightly harder to predict.

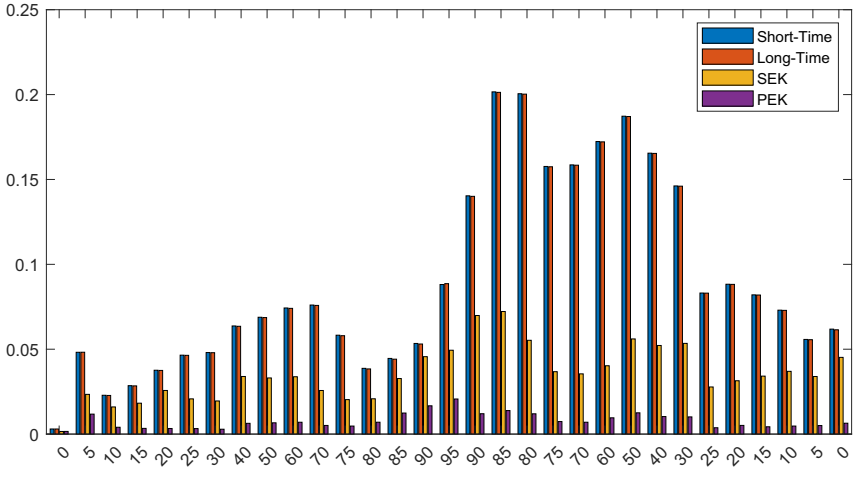

Figure 7: The average RMSEs values on average over 12 specimens (3 replicates for each of the 4 specimen types). It becomes clearer how hard it is for Fickian models to represent desorption or high RHs and combining them is even worse.

the RMSE representations emphasizes even more where the errors are large or small.

The precision of the PEK model fits decreases at higher RH, especially in adsorption but it is also notable for desorption. This phenomenon can for example be seen in Figure 7. Crank (1975) and Willems (2022) might have an explanation for this phenomenon when the involved heat exchange of MC-changes limits the sorption rates. That is, however, out of the scope of this paper.

All models showed smaller RMSE in adsorption than in desorption even if PEK has the worst performance for high-RH-adsorption (Figure 7).

Generally, it is hard for the models to represent the MC curves at a high RH level for desorption. The Fickian-based models perform significantly poorly at high RH levels for desorption.

Welded wood seems to be more Fickian in its properties. One possible explanation is that due to the rigidity of the welded bond line, the welded joints swell less. In general, welded wood seems more suitable for the models used. The residuals are smaller than for unwelded wood.

Moreover, the RMSEs for pine and welded pine are slightly larger than those for beech and welded beech.

It is recommended for future work to investigate how welding parameters can affect the vapor sorption properties of the welded wood.

4 Conclusions

The PEK model fits more precisely than the other studied models to the MC curves, particularly in adsorption. Nevertheless, the slightly higher RMSEs for the PEK at higher RH reveal that probably other phenomena simultaneously happen with water adsorption that this model cannot fully cover.

Author contributions: All the authors have accepted responsibility for the entire content of this submitted manuscript and approved submission.
Research funding: None declared.
Conflict of interest statement: The authors declare no conflicts of interest regarding this article.

Appendix

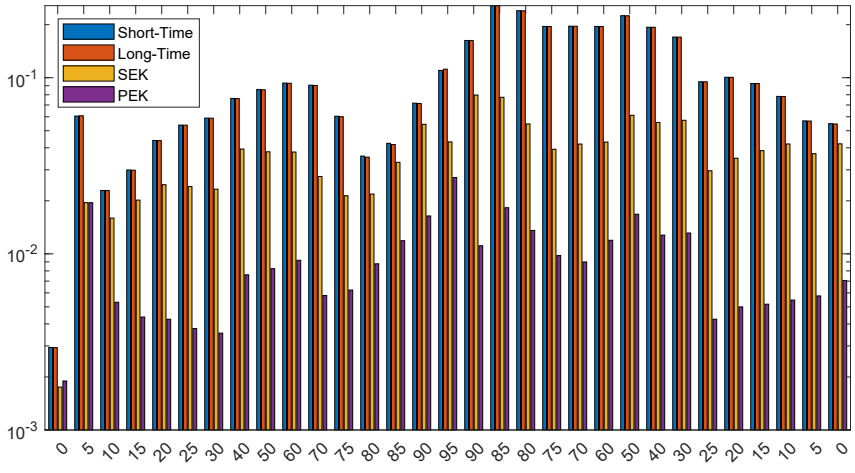

Figure A1: The average RMSE values of the model fits to the kinetic data in adsorption–desorption for three beech replicates.

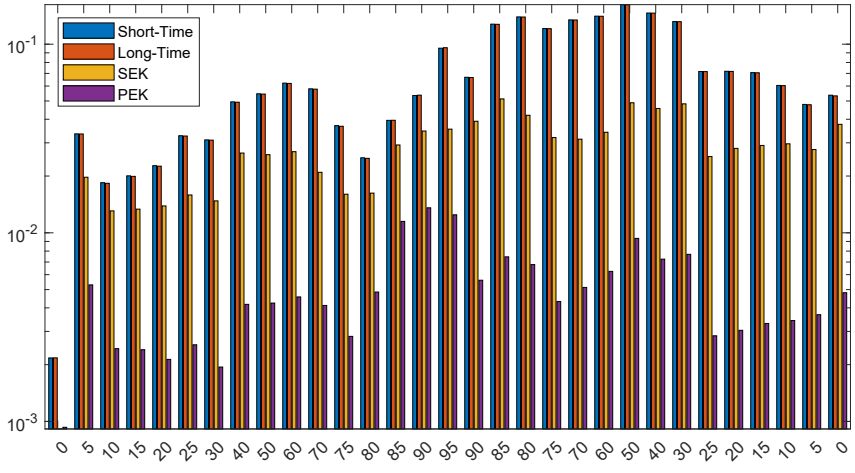

Figure A2: The average RMSE values of the model fits to the kinetic data in adsorption–desorption for three welded beech replicates.

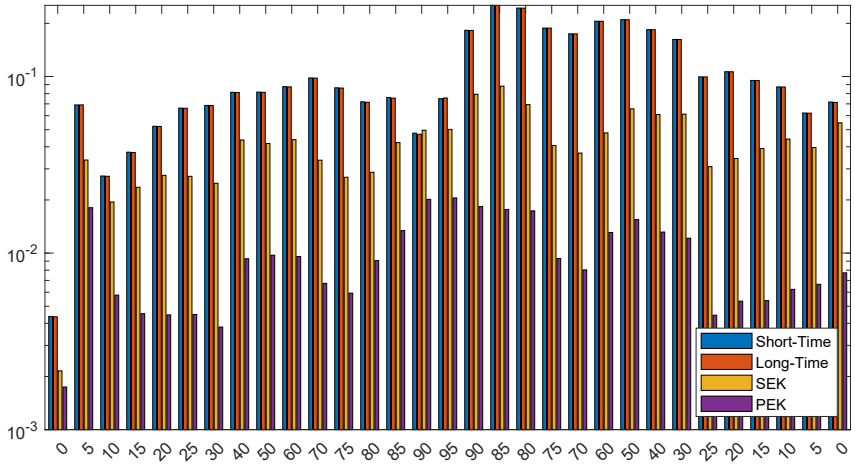

Figure A3: The average RMSE values of the model fits to the kinetic data in adsorption–desorption for three pine replicates.

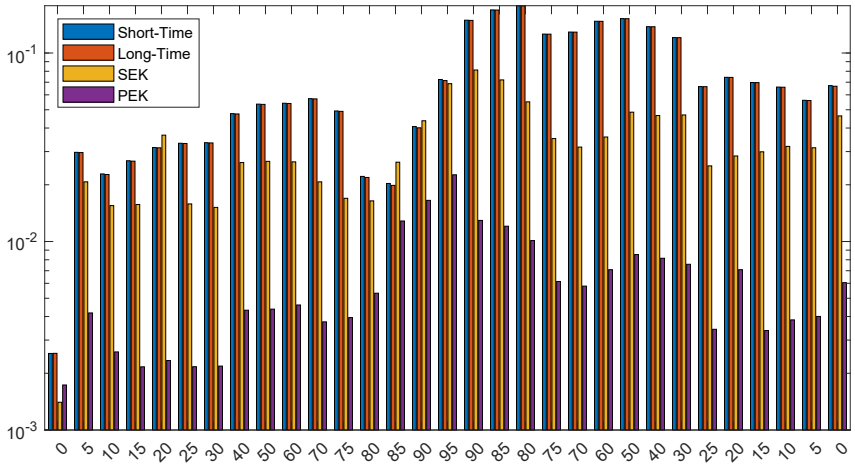

Figure A4: The average RMSE values of the model fits to the kinetic data in adsorption–desorption for three welded pine replicates.

References

Avramidis, S. (2007). Bound water migration in wood. In: Perré, P. (Ed.), *Fundamentals of wood drying*. A.R.BO.LOR, Nancy, France, pp. 105–124.

Belbekhouche, S., Bras, J., Siqueira, G., Chappey, C., Lebrun, L., Khelifi, B., Marais, S., and Dufresne, A. (2011). Water sorption behaviour and gas barrier properties of cellulose whiskers and microfibrils films. Carbohydr. Polym. 83: 1740–1748.

Berger, J., Colinart, T., Loiola, B.R., and Orlande, H.R. (2020). Parameter estimation and model selection for water sorption in a wood fibre material. Wood Sci. Technol. 54: 1423–1446.

Crank, J. (1975). *The mathematics of diffusion*, 2nd ed. Oxford: Clarendon.

Fick, A. (1855). On liquid diffusion. Phil. Mag. J. Sci. 10: 30–39.

Glass, S.V., Boardman, C.R., and Zelinka, S.L. (2017). Short hold times in dynamic vapour sorption measurements mischaracterize the equilibrium moisture content of wood. Wood Sci. Technol. 51: 243–260.

Glass, S.V., Boardman, C.R., Thybring, E.E., and Zelinka, S.L. (2018). Quantifying and reducing errors in equilibrium moisture content measurements with dynamic vapour sorption (DVS) experiments. Wood Sci. Technol. 52: 909–927.

Grönquist, P., Frey, M., Keplinger, T., and Burgert, I. (2019). Mesoporosity of delignified wood investigated by water vapour sorption. ACS Omega 4: 12425–12431.

Hill, C.A.S., Norton, A., and Newman, G. (2010a). The water vapour sorption behaviour of flax fibers–analysis using the parallel exponential kinetics model and determination of the activation energies of sorption. J. Appl. Polym. Sci. 116: 2166–2173.

Hill, C.A.S., Norton, A., and Newman, G. (2010b). Analysis of the water vapour sorption behaviour of Sitka spruce [*Picea sitchensis* (Bongard) Carr.] based on the parallel exponential kinetics model. Holzforschung 64: 469–473.

Hill, C.A.S., Norton, A., and Newman, G. (2010c). The water vapour sorption properties of Sitka spruce determined using a dynamic vapour sorption apparatus. Wood Sci. Technol. 44: 497–514.

Hill, C.A.S., Moore, J., Jallaludin, Z., Leveneu, M., and Mahrdt, E. (2010d). The influence of earlywood/latewood and ring position upon the water vapour sorption properties of Sitka spruce. Int. Wood Prod. J. 2: 12–19.

Jalaludin, Z., Hill, C.A.S., Samsi, H.W., Husain, H., and Xie, Y. (2010). Analysis of water vapour sorption of oleo-thermal modified wood of Acacia mangium and Endospermum malaccense by a parallel exponential kinetics model and according to the Hailwood–Horrobin model. Holzforschung 64: 763–770.

Keey, R.B., Langrish, T.A.G., and Walker, J.C.F. (1999). *Kiln-drying of lumber*. Springer-Verlag, Berlin, Heidelberg, New York, p. 326.

Kohler, R., Renate, D., Bernhard, A., and Rainer, A. (2003). A numeric model for the kinetics of water vapour sorption on cellulosic reinforcement fibers. Compos. Interfaces 10: 255–257.

Kohler, R., Alex, R., Brielmann, R., and Ausperger, B. (2006). A new kinetic model for water sorption isotherms of cellulosic materials. Macromol. Symp. 244: 89–96.

Okubayashi, S., Griesse, U.J., and Bechtold, T. (2004). A kinetic study of moisture sorption and desorption of lyocellfibers. Carbohydr. Polym. 58: 293–299.

Okubayashi, S., Griesser, U.J., and Bechtold, T. (2005a). Water accessibilities of man-made cellulosic fibers effects of fiber characteristics. Cellulose 12: 403–410.

Okubayashi, S., Griesser, U.J., and Bechtold, T. (2005b). Moisture sorption/desorption behaviour of various manmade cellulosic fibers. J. Appl. Polym. Sci. 97: 1621–1625.

Papadopoulos, A.N. and Hill, C.A.S. (2003). The sorption of water vapour by anhydride modified softwood. Wood Sci. Technol. 37: 221–231.

Pfriem, A., Zauer, M., and Wagenfuhr, A. (2010). Alteration of the unsteady sorption behaviour of maple (*Acer pseudoplatanus* L.) and spruce (*Picea abies* (L.) Karst.) due to thermal modification. Holzforschung 64: 235–241.

Popescu, C.M. and Hill, C.A.S. (2013). The water vapour adsorption– desorption behaviour of naturally aged Tilia cordata Mill. wood. Polym. Degrad. Stabil. 98: 1804–1813.

Popescu, C.M., Hill, C.A.S., Curling, S., Ormondroyd, G., and Xie, Y. (2014). The water vapour sorption behaviour of acetylated birch wood: how acetylation affects the sorption isotherm and accessible hydroxyl content. J. Mater. Sci. 49: 2362–2371.

Salin, J.G. (2010). Problems and solutions in wood drying modeling: history and future. Wood Mater. Sci. Eng. 5: 123–134.

Sharratt, V., Hill, C.A.S., Zaihan, J., and Kint, D.P.R. (2010). Photodegradation and weathering effects on timber surface moisture profiles as studied using dynamic vapour sorption. Polym. Degrad. Stab. 95: 2659–2662.

Sparr, G. and Sparr, A. (2000). *Kontinuerliga system*. Studentlitteratur, Sweden.

Stamm, A.J. (1964). *Wood and cellulose science*. The Ronald Press Company, New York, p. 549.

Thybring, E.E., Boardman, C.R., Glass, S.V., and Zelinka, S.L. (2019a). The parallel exponential kinetics model is unfit to characterize moisture sorption kinetics in cellulosic materials. Cellulose 26: 723–735.

Thybring, E.E., Glass, S.V., and Zelinka, S.L. (2019b). Kinetics of water vapour sorption in wood cell walls: state of the art and research needs. Forests 10: 704.

Van der Wel, G.K. and Adan, O.C.G. (1999). Moisture in organic coatings: a review. Prog. Org. Coat. 37: 1–14.

Vaziri, M. (2011). Water resistance of Scots pine joints produced by linear friction welding. Ph.D. thesis. Skellefteå, Luleå University of Technology.

Vaziri, M., Dreimol, C., Abrahamsson, L., Niemz, P., and Sandberg, D. (2023). Water-vapour sorption of welded bond-line of European beech and Scots pine. Holzforschung 77, It is published now.

Willems, W. (2022). Improved boundary conditions for models of coupled heat and water vapour transfer between an adsorbent and the ambient. Int. J. Therm. Sci. 172: 107296.

Xie, Y., Hill, C.A.S., Jalaludin, Z., and Sun, D. (2011). The water vapour sorption behaviour of three celluloses: analysis using parallel exponential kinetics and interpretation using the Kelvin–Voigt viscoelastic model. Cellulose 18: 517–530.

Zelinka, S.L., Glass, S.V., and Thybring, E.E. (2018). Myth versus reality: do parabolic sorption isotherm models reflect actual wood-water thermodynamics? Wood Sci. Technol. 52: 1701–1706.